


HPMA-PLGA Based Nanoparticles for Effective *In Vitro* Delivery of Rifampicin

Sarita Rani¹ · Avinash Gothwal¹ · Pawan K. Pandey¹ · Devendra S. Chauhan² · Praveen K. Pachouri² · Umesh D. Gupta² · Umesh Gupta¹ 

Received: 24 August 2018 / Accepted: 8 November 2018 / Published online: 3 December 2018
© Springer Science+Business Media, LLC, part of Springer Nature 2018

ABSTRACT

Purpose Tuberculosis (TB) chemotherapy witnesses some major challenges such as poor water-solubility and bioavailability of drugs that frequently delay the treatment. In the present study, an attempt to enhance the aqueous solubility of rifampicin (RMP) was made via co-polymeric nanoparticles approach. HPMA (N-2-hydroxypropylmethacrylamide)-PLGA based polymeric nanoparticulate system were prepared and evaluated against *Mycobacterium tuberculosis* (MTB) for sustained release and bioavailability of RMP to achieve better delivery.

Methodology HPMA-PLGA nanoparticles (HP-NPs) were prepared by modified nanoprecipitation technique, RMP was loaded in the prepared NPs. Characterization for particle size, zeta potential, and drug-loading capacity was performed. Release was studied using membrane dialysis method.

Results The average particles size, zeta potential, polydispersity index of RMP loaded HPMA-PLGA-NPs (HPR-NPs)

were 260.3 ± 2.21 nm, -6.63 ± 1.28 mV, and 0.303 ± 0.22 , respectively. TEM images showed spherical shaped NPs with uniform distribution without any cluster formation. Entrapment efficiency and drug loading efficiency of HPR-NPs were found to be $76.25 \pm 1.28\%$, and $26.19 \pm 2.24\%$, respectively. Kinetic models of drug release including Higuchi and Korsmeyer-peppas demonstrated sustained release pattern. Interaction studies with human RBCs confirmed that RMP loaded HP-NPs are less toxic in this model than pure RMP with ($p < 0.05$).

Conclusions The pathogen inhibition studies revealed that developed HPR-NPs were approximately four times more effective with ($p < 0.05$) than pure drug against sensitive *Mycobacterium tuberculosis* (MTB) stain. It may be concluded that HPR-NPs holds promising potential for increasing solubility and bioavailability of RMP.

KEYWORDS

HPMA (N-2-hydroxypropylmethacrylamide) · nanoparticles (NPs) · PLGA · rifampicin (RMP) · solubility · tuberculosis (TB)

Highlights

- HPMA (N-2-hydroxypropylmethacrylamide) co-polymer was synthesized and characterized.
- HPMA-PLGA NPs were allowed to self-assemble in order to remove acetonitrile, organic solvent for safety purposes.
- Solubility of RMP was increased 65 folds via HPMA-PLGA hydrophilic co-polymer.
- Overall efficacy of the prepared polymeric nanoparticles against the *Mycobacterium tuberculosis* was enhanced several folds over the naïve drug RMP.

✉ Umesh Gupta
umeshgupta175@gmail.com; umeshgupta@curaj.ac.in; <https://www.curaj.ac.in>

¹ Department of Pharmacy, School of Chemical Sciences and Pharmacy Central University of Rajasthan, Bandarsindri Ajmer, Rajasthan 305817, India

² ICMR-National JALMA Institute for Leprosy and Other Mycobacterial Diseases, Tajganj, Agra, Uttar Pradesh 282001, India

ABBREVIATIONS

| | |
|---------|--|
| ACN | Acetonitrile |
| ETB | Ethambutol |
| HPMA | N-2-hydroxypropylmethacrylamide co-polymer |
| HP-NPs | HPMA-PLGA nanoparticles |
| HPR-NPs | Rifampicin loaded HPMA-PLGA nanoparticles |
| INH | Isoniazid |
| MABA | Microplate Alamar Blue Assay |
| MTB | <i>Mycobacterium tuberculosis</i> |
| MIC | Minimum inhibitory concentration |
| NPs | Nanoparticles |
| PLGA | Poly-lactic-co-glycolic acid |
| PNPs | Polymeric Nanoparticles |
| PPB | Plasma protein binding |
| PYZ | Pyrazinamide |

| | |
|-----|----------------------------------|
| RMP | Rifampicin |
| STP | Streptomycin |
| TB | Tuberculosis |
| TEM | Transmission electron microscopy |
| WHO | World Health Organization |

INTRODUCTION

After HIV-AIDS, TB is second most serious infectious disease comes from a single causative organism, *Mycobacterium tuberculosis* (MTB). Global efforts have been successful in reducing the mortality rate of TB patients by 37% and have saved approximately 53 million lives since 2000 (1). Despite this achievement, TB remains a severe threat to global health. According to World Health Organization (WHO) TB report 2017, 10.4 million people were infected with TB in 2016; 5.9 (56%) million men, 3.5 (34%) million women and 1.0 (10%) million children. Globally, 11% of the 1.2 million new TB cases in 2016 were HIV-positive. The slow-growing acid-fast bacilli, MTB infects lungs, spleen, brain, kidneys and other organs (2). WHO established guidelines that duration of TB therapy is 9 months for adults and 12 months for children. TB chemotherapy includes first and second-line drugs. Isoniazid (INH), rifampicin (RMP), pyrazinamide (PYZ), ethambutol (ETB), streptomycin (STP) are first-line drugs and kanamycin, amikacin including with other antibiotics comes in list of second-line drugs. The daily doses are required in different phases of treatment. TB chemotherapy consists of two phases (intensive and continuous). In intensive phase; patients takes INH, RMP, PYZ and ETB in different doses, while in continuous phase INH and RMP are given in combination. Initially, INH is responsible for killing 95% TB bacteria and then RMP, PYZ replaces its role during the intensive phase of therapy. The chemotherapy duration prolonged by 12–18 months if INH or RMP not given to patients. Hence, both INH and RMP play an important role in the TB chemotherapy (3–5). When bacteria become multidrug resistant, the antibiotic therapy competence gradually decreases. The antibiotic chemotherapy will be used for six months in case of multidrug resistance and toxicity of antibiotics will increase (6). Patient non-compliance adds further complications in the TB treatment as multiple doses would be administered on a daily basis or weekly not less than six months according to WHO guidelines. To enhance the patient compliance, nanotechnology including polymeric nanoparticles (PNPs) (7) has been adopted for drug entrapment and release (8). However, organic solvents and some hazardous chemicals used in manufacturing, limit the utility of drugs. NPs drug delivery is a promising approach to improve the solubility of hydrophobic drugs and their bioavailability (9). The small size of PNPs carriers may lead to the cellular uptake of drug and allow efficient drug accumulation in the body at the targeted

sites. MTB predominantly resides intracellularly in macrophages and phagocytic cells accessed by the systemic vascular blood supply by phagocytosis (10). From the previous studies, it was observed that NPs of 1000 nm size, moving in the blood circulation could be easily phagocytized by the MTB-infected macrophages. In the nanoparticulate system, drug starts releasing after administration and then moves into the infected cells in a controlled manner (11). The polymer poly (lactic-co-glycolic acid) (PLGA) gained the attention of researchers because of its desirable drug delivery (12). PLGA is one of the most useful biodegradable polymer which produces two metabolic monomer units, i.e., lactic acid and glycolic acid after hydrolysis. These two monomer units are endogenous and metabolized by the kreb's cycle (13). The attractive properties such as sustained drug release effect, biodegradability, and biocompatibility make this polymer, a suitable candidate for drug delivery. The matrix of this polymer prevents degradation of drugs and maintains release kinetics of the drugs from NPs.

In the last 30 years, N-(2-hydroxypropylmethacrylamide) (HPMA) (Fig. 1 (a) co-polymer extensively studied for drug delivery system. Polymeric conjugates of this co-polymer improved the aqueous solubility, bioavailability, and therapeutic efficacy of many drugs. HPMA is a potential amide copolymer recognized to reduce toxicity and decrease the multi drug resistance (14). More than two HPMA copolymer-drug conjugates are in the investigation phase of clinical trials (15). Safety and lack of immunogenicity are the essential properties of HPMA copolymer. A conjugate of HPMA with different therapeutic agents or imaging probes has been reported (16). HPMA possesses a number of advantages for polymeric drug delivery system over conventional delivery methods. Primarily, it prolonged the half-life of low MW payloads with potential efficacy. It gained much attention in solubilizing the poor aqueous soluble drugs. Polymer conjugation prevents the premature metabolism of some drugs carriers before their distribution to the targeted sites (17–19).

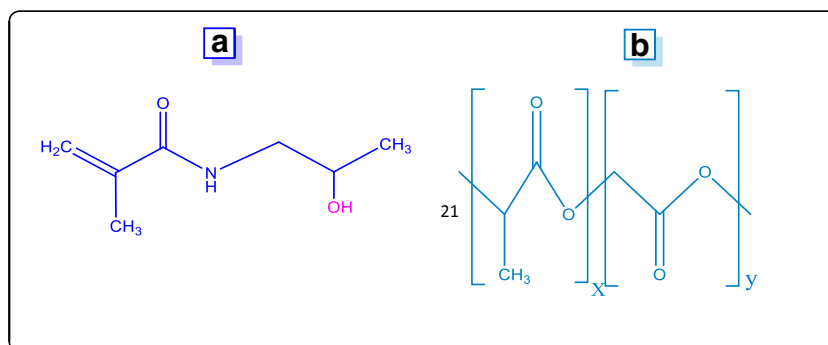
In the present study, amide copolymer HPMA and PLGA (Fig. 1 (b) based NPs were prepared using a surfactant lecithin. RMP was physically entrapped in the prepared NPs and evaluated for anti-TB effectivity against drug sensitive strains of *Mycobacterium tuberculosis* and safety as well. The intent of this research work was to improve the solubility of RMP and to deliver it safely with improved and sustained effect for the better treatment of TB and related pulmonary disease.

MATERIALS AND METHODS

Materials

Rifampicin (BP), also called Rifampin (USP) was a gift from Kwaliti Pharmaceuticals Ltd., India. Methacryloyl chloride,

Fig. 1 (a) Chemical structure of HPMA (N-2-hydroxypropylmethacrylamide); (b) Chemical structure of PLGA (x is the number of lactic acid units and y is the number of glycolic acid units).



aminopropan-2-ol, and lecithin were purchased from Alfa Aesar Pvt. Ltd., India. Anhydrous sodium carbonate and methylene chloride were purchased from TCI Chemicals Pvt. Ltd. India. PLGA was purchased from Sigma-Aldrich India. 96 well microplates were purchased from Tarsons Pvt. Ltd., India. Alamar blue dye and 7H9GC Middlebrook media were procured from Hi-media Laboratories Pvt. Ltd., Mumbai, India. Tween-80 was purchased from Spectrochem Pvt. Ltd. Mumbai, India. All other chemicals and reagents used were of analytical grade.

Synthesis of N-(2-Hydroxypropyl) Methacrylamide (HPMA)

HPMA was synthesized using a previously reported method (20). A quantity of 0.36 mL (0.95 mmol) 1-aminopropanol-2-ol was dissolved in 5 mL of methylene chloride. An accurately weighed anhydrous sodium carbonate 100 mg (0.95 mmol) was suspended in the above solution Fig. 2 (a) at 0°C. Then, a solution of 98.80 mg methacryloyl chloride in 5 mL methylene chloride was prepared and added drop wise under cooling with vigorous stirring. The assembly was left for stirring at 15°C for 1 h. Anhydrous sodium sulfate was added to absorb the moisture from the product and vacuum dried the solid after filtration. Then the solid product was dissolved in methylene chloride and kept in the deep freezer at -20°C. At last, a white crystalline solid product, HPMA was obtained after recrystallizing with acetone. The synthesized HPMA was confirmed by FT-IR spectrum and ¹H-NMR spectrum.

Characterization of Synthesized HPMA Copolymer

FT-IR Spectroscopy. FT-IR was performed at The Material Research Centre, MNIT, Jaipur, India for characterization of the copolymer. Pure RMP FT-IR spectrum was obtained by using KBr pellet on a Perkin Elmer FT-IR spectrophotometer supported by (PerkinElmer Spectrum™ software (M/Perkin Elmer, Inc. Waltham, Massachusetts, USA).

Proton Nuclear Magnetic Resonance (¹H-NMR) Spectroscopy. ¹H-NMR spectrum was recorded in the CDCl₃ solvent by

Bruker Ascend 500.3 MHz NMR spectrometer, Switzerland (7.269 ppm for ¹H-NMR as internal standard). The ¹H-NMR analysis was performed at School of Chemical Sciences and Pharmacy, Central University of Rajasthan, Bandarsindri, Rajasthan, India.

Synthesis of RMP Loaded HPMA-PLGA Nanoparticles

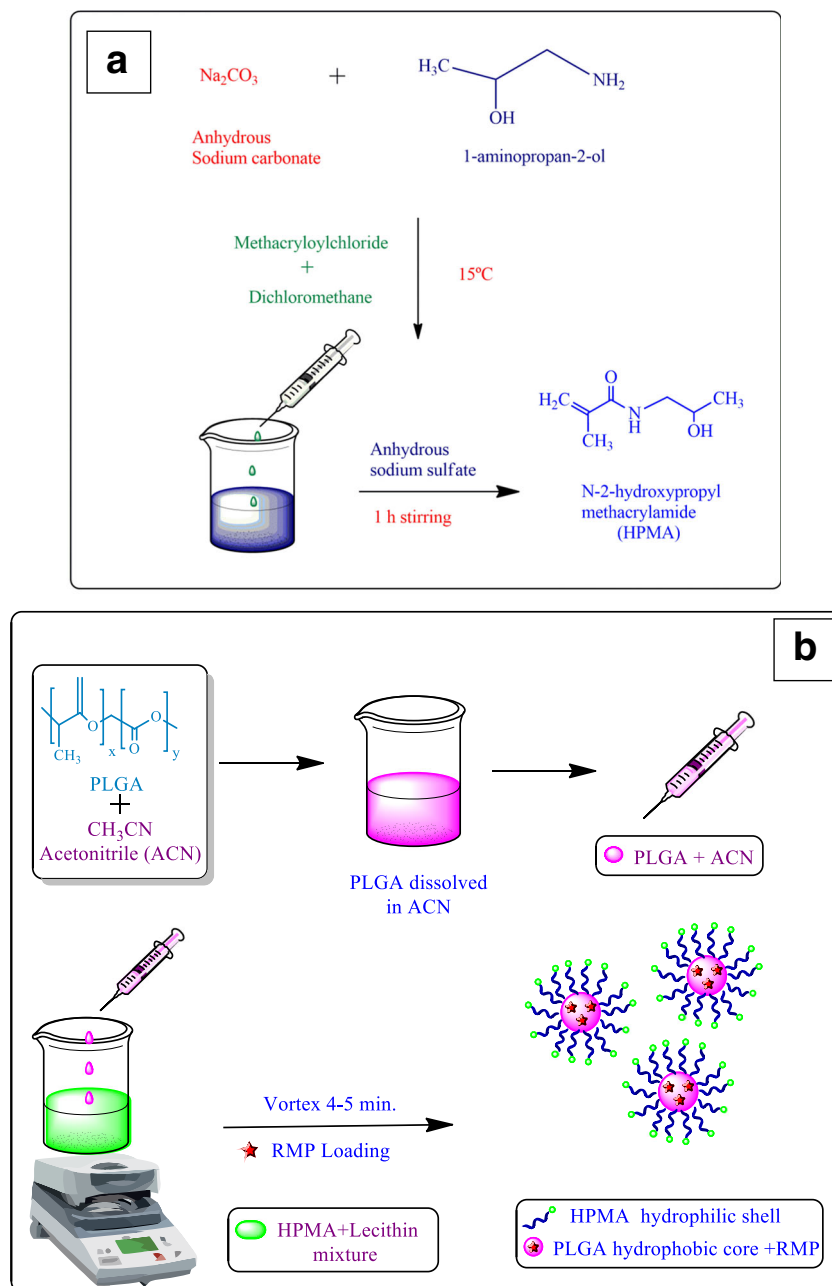
HP core-shell NPs were synthesized from HPMA copolymer, PLGA and soybean phosphatidylcholine lecithin using a modified nano-precipitation technique (21) Fig. 2 (b). Briefly, 1.0 g (0.011 mmol) PLGA was dissolved in acetonitrile (ACN). Lecithin and HPMA (7:3 M ratio) were dissolved in 4% aqueous solution of ethanol and heated to 65°C, separately. The PLGA solution was added to the preheated lipid via syringe drop-wise (1 mL/min) with gentle stirring. HP-NPs were allowed to self-assemble for 6 h with continuous stirring and the organic solvent was evaporated during self-assembling process. Tomcin *et al.* also reported that the solvent evaporation step was followed to avoid hazardous properties/ harmful effects of organic solvent (22). Whatman filter paper of size no. 41 was used for further washing of NPs solution to remove the impurities. The prepared HP-NPs were stored at 4°C for future use.

Similarly, RMP loaded HP-NPs were prepared following the similar method and the suitable quantity of the drug was added to acetonitrile, and the solution was further added to HPMA-PLGA solution of ACN with stirring at room temperature. In addition, the solution was placed in an end-sealed dialysis bag (5000 Da, MWCO, Hi-Media, India) and put in 50 mL distilled water for dialysis process. After 36 h of dialysis, the solution was centrifuged, lyophilized followed by getting a solid product of HPR-NPs formulation.

Concentration-Dependent Solubilization Study

In this study, a comparison of solubility of RMP and HPR-NPs was done. Briefly, RMP (1 mg) was dissolved in 100 mL water, and a subsequent calibration curve was prepared by following membrane filtration in the range of 1–10 µg/mL using methanol as co-solvent. The absorbance was taken by

Fig. 2 (a): Schematic representation of HPMA co-polymer synthesis and; **(b)** Schematic method of preparation of HPR-NPs.



UV double beam spectrophotometer at 333 nm. The phase solubility analysis of HPR-NPs was performed with increasing co-polymer concentration range. The experiments were performed in triplicate, data was represented as mean, and standard deviation subsequently subjected to statistical analysis as described in section 2.11.

Characterization of HPR-NPs

Size, Zeta Potential and Polydispersity Index (PDI)

Zeta sizer (Nano ZS, Malvern, UK) measured the electrophoresis mobility, average particle size, zeta potential and size

distribution of prepared HPR-NPs and HP-NPs. For size analysis, 1 mL of prepared NPs were diluted with 4 mL de-ionized water at 25°C by light scattering at 90° angle. Each data value represents an average of three measurements. Highly poly-dispersed samples, containing particles with different sizes, will show a high polydispersity index value near to 1. A low PDI close to 0 was desirable. The PDI was determined by considering the above mentioned concept.

Electron Microscopy (Transmission Electron Microscopy)

TEM characterized the size and surface morphology of NPs. A drop of prepared HPR-NPs was placed over a 400-mesh

carbon-coated copper grid. NPs solution drop was spread on a degreased glass plate uniformly for sample preparation. Then negatively stained with phosphotungstic acid solution (3%, *w/v*, adjusted to pH 4.7 with KOH) with an accelerating voltage of 95 kV. The grids were washed twice with distilled water and air-dried earlier to capture images with the help of the computer.

Drug Entrapment Efficiency and Percent Drug Loading

For determining entrapment efficiency (EE) and percent drug loading (DL), 2 mg HPR-NPs were dissolved in ACN (10 mL), and the solution was centrifuged (Remi 4-RC-DX, India) for 15 min at 1500 RPM and filtered using membrane filter

(0.22 μ , Rankem, India). The filtrate was collected and quantified by UV-visible spectrophotometer (Double Beam UV-Vis Spectrophotometer, LT-2800, Labtronics, India) at 333 nm for RMP. Free RMP, was removed by placing the solution, in the end sealed dialysis membrane bag (MWCO = 5000 Da, Hi-Media, India) in 250 mL distilled water with overnight stirring. The NPs were purified by dialysis method. The percentage drug EE and DL was determined by eq. 1 and eq. 2 respectively. A previously reported protocol with slight modification was used for determining the entrapment efficiency of HPR-NPs (23). The formulated nanoparticulate suspension was centrifuged (Remi centrifuge, India) at 4–5°C for one h. The formulation was freeze-dried after discarding the supernatant. The NPs yield was calculated by using eq. 3.

$$EE (\%) = \frac{\text{Amount of drug used in formulation} - \text{amount of unbound drug}}{\text{Amount of drug used in formulation}} \times 100 \quad (1)$$

$$DL (\%) = \frac{\text{Weight of RMP added}}{\text{Total amount of polymer and drug added}} \times 100 \quad (2)$$

Nanoparticles yield

$$= \frac{\text{Amount of recovered HP-NPs}}{\text{Total amount of polymer and drug added}} \quad (3)$$

Protein Binding Study

Equilibrium retro-dialysis method was performed to evaluate the plasma protein binding of HPR-NPs (24). Initially, four mL plasma was added in 2 mL HPR-NPs solution and kept aside for 30 min. in dialysis (5000 Da; Hi-Media) bag and placed in a glass beaker with 120 ± 30 rpm magnetic stirring (Remi, India) at room temperature. Then, 0.5 mL of 5% glucose filled in dialysis bags and kept into the same glass beaker then retro-dialysis was done for 6 h with 120 ± 30 rpm magnetic stirring. Volume was made up with distilled water. Samples of plasma (200 μ l) and dialysate were collected and analyzed using a UV-visible spectrophotometer. The % PPB of RMP and INH was calculated as:

$$\%PPB = 5.2 \times C_o C_i / 0.5 \times C_i + 5.2 \times C_o \times 100\%$$

Here,

C_o drug concentrations in the plasma outside the dialysis bags.

C_i dialysate inside the dialysis bags (mg/mL).

The values 0.5 and 5.2, represents inside solution volume and outside the dialysis bags respectively (mL).

In Vitro Release

RMP released from the NPs were evaluated by dispensing the HPR-NPs in PBS buffer 7.4 pH medium containing ascorbic acid (prevent oxidative degradation of drugs in dialysis method). Briefly, accurately weighed 2 mg of HPR-NPs solution was taken in a dialysis bag (MWCO = 5000 Da, Hi-Media, India) and the dialysis bag was end-sealed and submerged fully into 50 mL of PBS buffer (pH 7.4) solution at 37°C with stirring at 120 rpm for 72 h. At predetermined time intervals, 2 mL aliquots were withdrawn filtered through 0.45 μ m syringe filter and replenished with an equal volume of fresh PBS buffer. The concentrations of RMP in samples were determined by UV-Vis double spectrophotometer. The amount of release RMP was analyzed by a UV spectrophotometer at 333 nm wavelength. Each measurement was taken three times for better results analysis. The *in vitro* release study was further planned by applying in different kinetic models such as zero, first, Higuchi, Hixon crowell, and Korsmeyer-Peppas model, etc.

Hemolysis Toxicity Study

The hemolytic study regarding percentage hemolysis was done to evaluate the HPR-NPs compatibility with RBCs (erythrocytes) compared to RMP (25). One mL of suitably diluted HPMA, PLGA, lecithin, HP-NPs, and HPR-NPs were added separately to 4 mL of normal saline and allowed to interact with RBCs suspension. Similar step was performed for drug solution and lecithin solution, mixed with 4 mL of normal saline, and allowed to interact with RBCs suspension. Supernatants were diluted with equal volume of normal saline and an absorbance was seen at 540 nm wavelength. Distilled

water was used as a control with hemolytic value as 100%. Percent hemolysis was thus determined for each sample, using the following equation

$$\% \text{Hemolysis} = \frac{[Ab_s]}{AB_{100}} \times 100$$

Ab_s Sample absorbance.

AB_{100} Absorbance of control without formulation.

Anti-TB Assay

Micro Plate Alamar Blue Assay (MABA)

MABA was performed with slight modification in the previously reported method (26). In outer peripheral wells of sterile 96-well plates, sterile deionized water (200 μL) was added to minimize the loss of medium during incubation. In each plate, 100 μL of 7H9GC broth was added in rows B to G in columns 2 to 11 (7H9 broth). The broth was prepared by this method: 2.35 g 7H9 broth was dissolved in deionized-autoclaved water followed by adding 2 mL of glycerol and autoclaved at 15 lbs., 121°C for 10 min and cooled at 45°C. At the end, 1 mL Middle brook ADC was added aseptically and mixed well before dispensing. The 100 μL of RMP solution was added from B to G rows (column 2, 3) to investigate the minimum inhibitory concentration (MIC) of pure drug. Then, 100 μL was transferred from column 3 to 4 and mixed the wells using a multichannel pipette. Similar serial dilutions (1:2) were done in columns 3 to 10, and simultaneously discarded the excess medium (100 μL) from wells (column 10) to get a final concentration range for RMP 4 $\mu\text{g}/\text{mL}$ to 0.015 $\mu\text{g}/\text{mL}$ in each 96 well plate. After that, 100 μL of sensitive *M. tuberculosis* strain (tested by 1% proportion method) were added in rows B to G (columns 2 to 11). Column 11 was considered as a control. Plates were sealed with parafilm and kept for incubation at 37°C for 5 days. On 5th day, 50 μL of a freshly prepared mixture of 10x Alamar Blue reagent (1:1) was added to well B11 and left to incubate at 37°C for 24 h after resealing with parafilm. All the wells would receive the Alamar dye if well B11 turned pink. The microplates were resealed with parafilm after adding Alamar dye in each test well and incubated for 24 h. A blue color was an indication of no growth and pink color indicated as growth. For the determination of MIC of the formulations, same procedure was applied. The wells, in rows B to G (columns 2 to 11) filled with 100 μL of 7H9GC broth. In rows, B to C 1000 μL of 2x HPMA solution was added and PLGA solution in D to E and HPR-NPs solutions in F to G in columns 2 and 3 respectively. Then, transferred 100 μL from column 3 to 4 and 4 to 5 through column 10 for the identical serial 1:2 dilution and mixed the wells content nicely and excess medium (100 μL) was discarded from the

wells in column 10. Now, the final concentration range was as: 0.4 to 0.0015 $\mu\text{g}/\text{mL}$ for HPMA solution, same for the PLGA and RMP in HPR-NPs 1 to 0.0078 $\mu\text{g}/\text{mL}$ in each well of plates. After that, 100 μL of sensitive *M. tuberculosis* strain (tested by 1% proportion method) was added to the test wells. The well B11 was taken as control/drug-free. Plates were left for incubation after resealing at 37°C for 5 days. At 5th day, 50 μL of a freshly prepared 10x Alamar Blue reagent was added to well B11. Then plates were again incubated at 37°C for 24 h. If B11 turned pink after that reagent, mixture was added to the wells of microplate. After adding Alamar dye in all the test wells, microplate was allowed to incubate for next 24 h at 37°C, and recorded the colors of all wells of microplate. A blue colour was an indication of no growth and pink colour indicated as growth. Moreover, the *M. tuberculosis* was examined under microscope without any treatment and at treated MIC of both RMP and HPR-NPs by fluorescence microscope (Olympus Inverted Fluorescence Microscope CKX53, Japan).

Microscopy

Microscopy was performed to investigate the growth of MTB, the heat fixed slides were prepared for growth control and determined MIC, stained with carbol-fuschin and again heated after 5 min, washed with water and decolorized with 25% sulphuric acid and kept for 2 min. In the last, slides were stained with 0.1% methylene blue and studied under the microscope (CX21FS1, Olympus Corporation, Tokyo, Japan) at different magnifications.

Statistical Treatment of Data

All data were expressed as means \pm standard deviation (SD) from at least three values. Student-tests, one way ANOVA Dunnett's Multiple Comparison tests and One way ANOVA Newman-Keuls Multiple Comparison Test were used for the statistical treatment of data using Graph Pad Prism (version 7.0, CA, USA) software, with $p < 0.05$ considered as significant.

RESULTS AND DISCUSSION

In recent years, PLGA with chitosan and alginate widely used for preparing a nanoparticulate formulation for reducing the dose frequency, patient non-compliance as well as the sustained release of TB frontline drugs. Terry *et al.* (27) also reported the sustained release formulation of RMP using PLGA polymer. HPMA co-polymer has unique characteristics to enhance the solubility of hydrophobic drugs and the overall efficacy of drugs too (28). Results from the present

study revealed that the solubility of RMP was increased several folds using HPMA.

Synthesis and Characterization of HPMA

HPMA co-polymer was synthesized by previously reported protocol (20). The calculated percent product yield was 85% with melting point 69–70°C. The obtained product was crystalline and white in colour with good yield after complete removal of residual organic solvents. The synthesis of HPMA was confirmed at each step with thin layer chromatography (TLC) and spectroscopic techniques (Fig. 3).

FT-IR and ¹H NMR Spectroscopy of HPMA

The synthesized HPMA was characterized by FT-IR and ¹H-NMR spectroscopy. In FT-IR spectrum, amide bond peak was seen at 1653.04 cm⁻¹. The sp³ carbon (alkyl/methyl group) and sp² carbon (alkenes) peak were appeared at 3299.74 cm⁻¹, and 2974.29 cm⁻¹ respectively in Fig. 3 (a). HPMA showed the characteristic shift for a proton of amide at 7.7 ppm (s, 1H, -CONH), of alcohol at 5.3 ppm (s,

1H, -OH) and methyl at 1.2 ppm (t, 3H, -C-CH₃), respectively Fig. 3 (b). The noticed peaks in FT-IR and ¹H-NMR confirmed the synthesis of HPMA. The synthetic pathway was simple, easy with high yield product during synthesis (Table I).

Preparation and Characterization of HP-NPs

RMP Loaded HP-NPs

HPMA provide electrostatic and steric stabilizations with longer circulation half-life of therapeutics *in vivo*. Functional-end group's attachment of targeting ligand such as antibodies, peptides and aptamers is the significant characteristic of HPMA. PLGA offer the hydrophobic core to encapsulate hydrophobic drugs. Lecithin provided a monolayer in the region of the hydrophobic core and act as emulsifying agent as well. The prepared HP-NPs were novel regarding the constitution and widely used HPMA co-polymer NPs were selected first time for this study. The percent nanoparticle yield of blank HP-NPs and HPR-NPs was calculated as 66.8 ± 1.24 and 64.16 ± 2.11 respectively. RMP loaded NPs were soluble in aqueous solution as observed in the solubilization study.

Fig. 3 (a) FT-IR spectra of co-polymer HPMA; (b) ¹H-NMR spectra of co-polymer HPMA

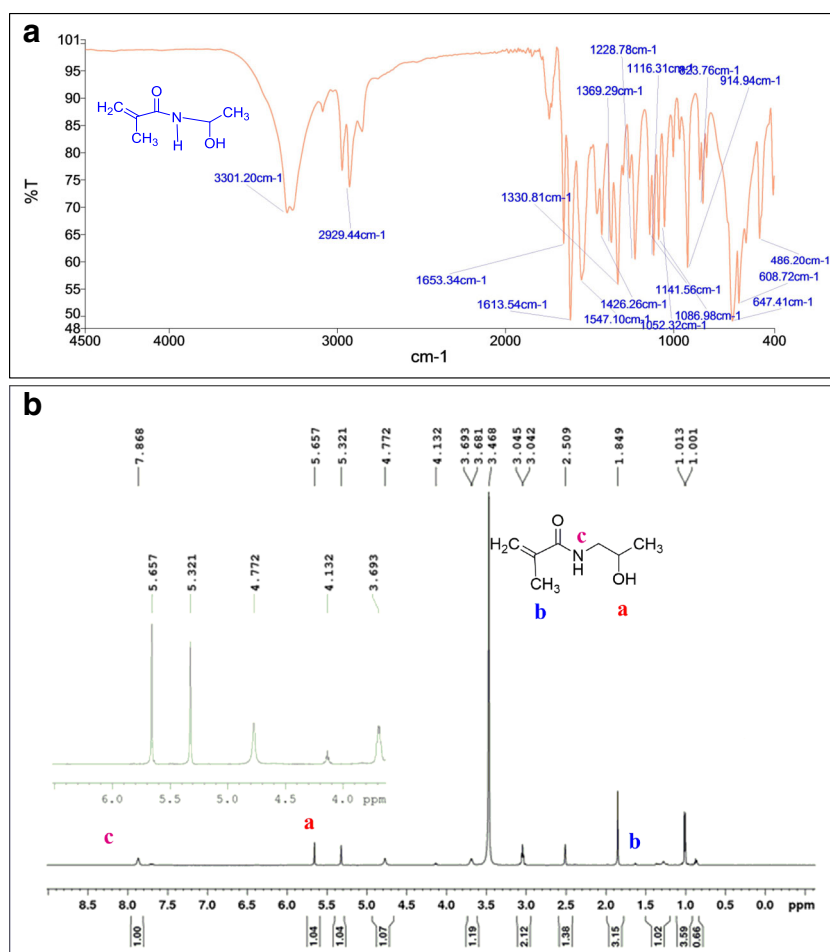


Table I Size, Zeta Potential, Entrapment Efficiency and Percent Yield for HP-NPs and HPR-NPs

| Formulation Code | Morphology | Size (nm) | Zeta potential (mV) | PDI | Entrapment efficiency (%) | Drug loading (%) | Percent Yield (%) |
|------------------|---------------------|--------------|---------------------|--------------|---------------------------|------------------|-------------------|
| HP-NPs | – | 184.4 ± 2.03 | -7.37 ± 1.23 | 0.265 ± 0.02 | – | – | 66.8 ± 1.24 |
| HPR-NPs | Spherical shape NPs | 260.3 ± 2.21 | -6.63 ± 1.28 | 0.303 ± 0.22 | 76.25 ± 1.28 | 26.19 ± 2.24 | 64.16 ± 2.11 |

The solubility studies results were explained in the section concentration dependent solubilization study.

Analysis of Size, Zeta Potential and PDI

The average particle size, zeta potential of HP-NPs were calculated as 184.4 ± 2.03 nm, -7.37 ± 1.23 mV while for HPR-NPs the obtained values were 260.3 ± 2.21 nm, -6.63 ± 1.28 mV, respectively (Table I). PDI of HP-NPs and HPR-NPs was determined 0.265 ± 0.02, 0.303 ± 0.22. PDI values were less than 1 which suggests that the prepared NPs have similar or uniform size particles with homogeneity. Zeta potential had minimal change after RMP loading which might be because of the state of polymers used in the research work. The slight increase in size was indirect evidence or indication for drug loading in HPR-NPs. Tomcin *et al.* reported NPs synthesized from HPMA with size range of 250–300 nm and described a method in which PNPs were stabilized by HPMA co-polymer for sustained drug release of poorly soluble drug (21).

Electron Microscopy

Transmission electron microscopy (TEM) was used to evaluate the morphology of prepared HPR-NPs. TEM images revealed that the PNPs have uniform spherical shell (Fig. 4) with size similar as obtained with particle size analysis. TEM images correspond to NPs with no agglomeration or collapse suggesting that particles of prepared formulations were remained unaggregated. The prepared PNPs were observed for the particle size and other properties to achieve the desired results *in vitro*.

Entrapment Efficiency and Drug Loading Efficiency

The percent EE and DL efficiency of HPR-NPs were 76.25 ± 1.28 and 26.19 ± 2.24 (Table I), respectively. The results suggested that the HPR-NPs were able to encapsulate drug in an excellent quantity. Results are supported by our previously reported work, in which EE of NPs can be more than 70%. In one of our earlier work, we reported PLGA-PEG copolymer nanoparticles as promising nanocarriers for anti-cancer drug-bendamustine. The entrapment efficiency exhibited by

PEGylated PLGA-bendamustine NPs was 52.3% (29) suggesting that the encapsulation of drug was substantial.

Concentration-Dependent Solubilization Study

RMP is a hydrophobic drug with 0.014–0.018 mg/mL solubility in distilled water. RMP bioavailability is unpredictable as compared to other first-line TB therapy drugs such as INH, PYZ, and ETH. Pelizza *et al.* reported that many factors affecting the solubility of RMP. One of the reason is that RMP shows polymorphism (30) and this affects the solubility of the drug, as many types of hydrates were seen during crystallography of RMP. Jindal *et al.* (31) studied the effect of particle size on the bioavailability and dissolution of RMP. It has been reported that the HPMA co-polymer increases the solubility of some hydrophobic drugs (17–19). Solubility study results revealed that solubility of RMP enhanced in a concentration-dependent manner of HPMA-PLGA co-polymer. In water, the maximum obtained solubility for RMP was 0.017 ± 0.002 mg/mL only, while the highest solubility at 50 µg/mL concentration of HPMA-PLGA in HPR-NPs was 1.056 ± 0.024 mg/mL (Fig. 5). There was an increase of almost 65 fold which was a highly significant result ($p < 0.05$). Therefore, the HPR-NPs were able to increase the aqueous solubility of RMP that might be due to the hydrophilic behavior of HPMA in HPMA-PLGA co-polymeric structure of the prepared HPR-NPs and might be the result of the formation of H-bond with HPMA co-polymer.

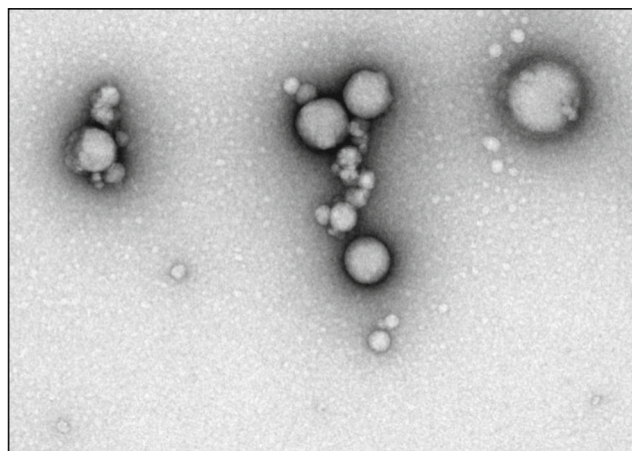


Fig. 4 Transmission electron microscopy (TEM) of RMP loaded HP-NPs.

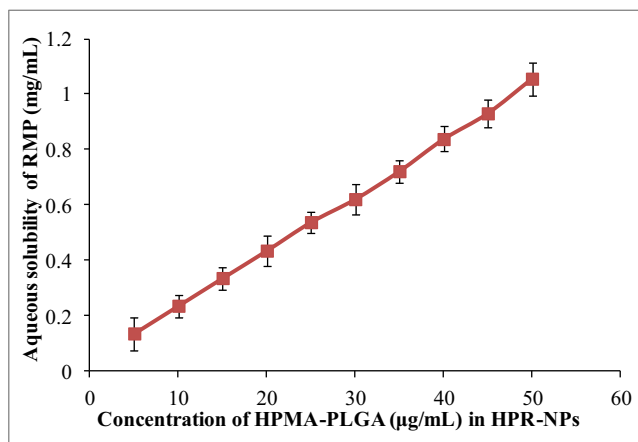


Fig. 5 Concentration dependent aqueous solubility of RMP using HPR-NPs. Values represents mean \pm SD ($n = 3$)

% Plasma Protein Binding (PPB)

The protein binding study was carried out using previously reported literature with slight modifications (21). %PPB of HPR-NPs was found to be $68 \pm 2.46\%$ which showed that the drug PPB rate was relatively high as the pure RMP (57–70%) (32). Briefly, equilibrium retro-dialysis was used to calculate the PPB of RMP encapsulated in HP-NPs. The binding efficiency depends on the structure, loading and physicochemical properties of the drug molecule (33). Moreover, the clearance from the body is also affected by protein binding (34). Hence, it can be hypothesized that the drug bioavailability, residence time of the drug will be higher and it will result in improving the overall effectivity.

In Vitro Drug Release

Membrane dialysis method in phosphate buffer saline pH 7.4 was used to study the *in vitro* release. This study revealed that pure RMP was released in a burst manner within an initial first hour and approximately 90% in 4 h. While the encapsulated RMP release was slower in case of HPR-NPs and continued up to 70 h and more Fig. 6 (a). *In vitro* release of RMP from HPR-NPs showed controlled release fashion up to 70 h while the pure drug released within 6 h (approximately 98%). To ensure that the release pattern was sustained or not it was decided to study the best-fit non-linear kinetics models (Fig. 6b and c). The obtained release kinetics was confirmed by Higuchi and Korsmeyer-Peppas model. The *in vitro* release of drug from HPR-NPs was easily explained by Korsmeyer-Peppas model Fig. 6 (b). The mathematical linear kinetic release modeling presented the highest linearity and was described as Korsmeyer-Peppas model and Higuchi Fig. 6 (c) model with $r^2 = 0.905$ (HPR-NPs) and $r^2 = 0.920$ (HPR-NPs), respectively. It also described the magnitude of release exponent N that explained that the release mechanism was

case-II relaxation release having stresses in hydrophilic polymers, which swell in water or biological fluids (35).

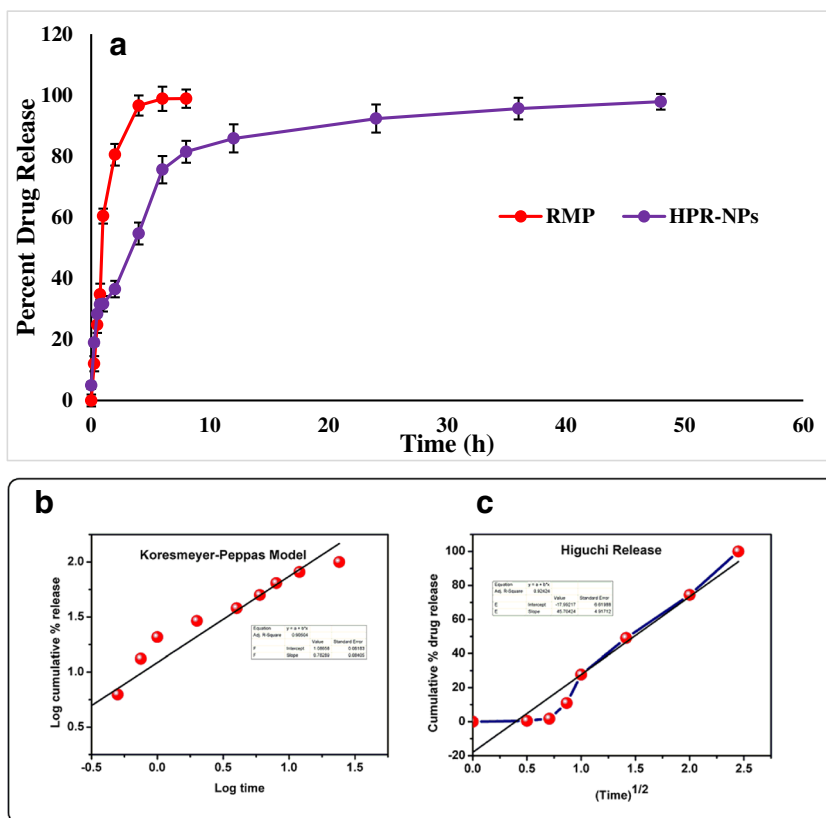
Hemolysis Toxicity Studies

The importance of safety and toxicity was addressed by accessing the compatibility and interactions of the developed nano-formulations with human RBCs. *Ex-vivo* hemolytic toxicity studies was done for HPMA, PLGA, RMP, lecithin, HP-NPs, and HPR-NPs. Percent hemolytic toxicity of RMP and HPR-NPs were observed as $33.4 \pm 0.45\%$ and 8.9 ± 0.25 (Fig. 7), respectively ($p < 0.05$). HPR-NPs showed four times less toxicity as compared to RMP which means the prepared NPs formulation reduced the toxicity of RMP. Additionally, the percent hemolytic toxicity of the synthesized HPMA was 3.62 ± 0.24 with ($p < 0.05$) which suggested that HPMA copolymer has less hemolytic toxicity in comparison to RMP. PLGA, HP-NPs and lecithin percent hemolysis were observed as 4.87 ± 0.17 , 4.41 ± 0.16 and $5.62 \pm 0.25\%$ ($p < 0.05$), respectively. The pure drug showed more toxicity as compared to PNP's formulation probably because of the reason that the hydrophobic drug RMP was completely encapsulated in the NPs and there was non-availability of the free drug for RBCs interaction.

Anti-TB Studies

Microplate Based Alamar Blue Assay (MABA) is one of the robust method to determine the inhibitory concentration of test formulations against *M. tuberculosis* bacterial (MTB) strain. The handling of the *M. tuberculosis* needs a sophisticated facility to carry out the experimentation, and hence, this was performed in the designated laboratory of Government of India, i.e., ICMR-National JALMA Institute for Leprosy and Other Mycobacterial Diseases, Tajganj, Agra, India. After 6 days, *M. tuberculosis* strain incubation tests results were recorded. After 5 days of incubation, the Alamar blue dye was added to the B11 (Growth control), MTB growth was confirmed by the change in color from blue to pink Fig. 8 (1). Dye was added simultaneously to rest of the wells and incubated for the next 24 h. Results were recorded on the following day. MIC of RMP for sensitive strain was recorded as $0.5 \pm 0.036 \mu\text{g/mL}$. The MIC value of HPR-NPs was found $\geq 0.125 \pm 0.02 \mu\text{g/mL}$ for the sensitive strain ($p < 0.05$), which was significantly lesser than the pure drug and showed four times more effective against the MTB strain Fig. 8 (2). Moreover, the microscopic examination of MTB revealed that HPR-NPs inhibited the MTB growth more significantly Fig. 8 (2) with respect to pure RMP, which might be due to the nanoparticulate delivery of RMP. Interestingly, we also observed the anti-TB activity for HPMA (MIC= $2.0 \pm 0.09 \mu\text{g/mL}$). We were unable to understand the obtained anti-TB activity in case of HPMA for which mechanism was

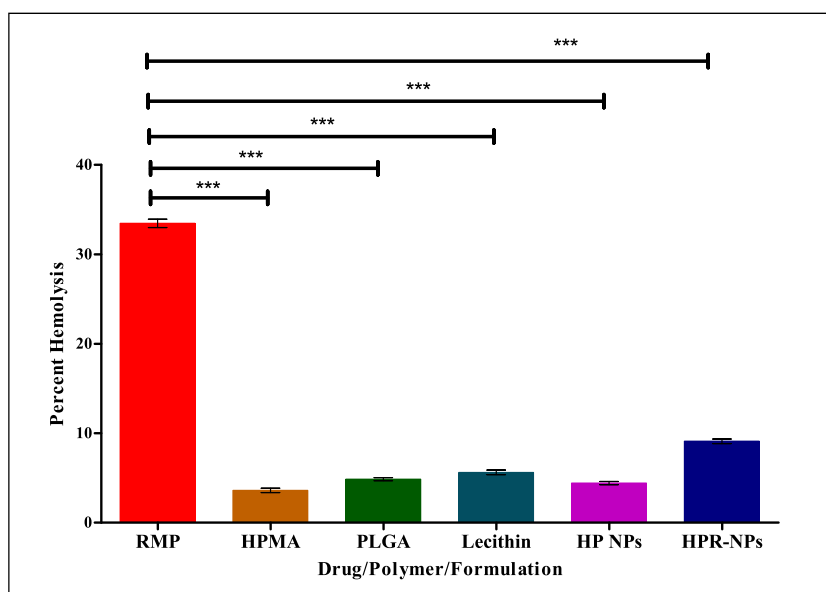
Fig. 6 *In vitro* drug release of RMP and HPR-NPs in PBS buffer (pH 7.4). The values represents mean \pm SD (n = 3). **(a)**; Graphical representation of Korsmeyer-Peppas kinetic release model **(b)**; Higuchi model for HPR-NPs **(c)**.



unpredictable Fig. 8 (2). Additionally, it can be clearly observed that the initial four wells of HPMA treated group in Fig. 8 (1b) were blue, indicating no growth suggesting that HPMA may have some anti-TB effect against the sensitive MTB strain. The previous reports also supports that the HPMA has some anti-infective activity (36). In the fluorescence images, it is clear that

the prepared formulations were more effective than pure anti-TB drug Fig. 8 (3). Microscopy also supported the results that the HPR-NPs showed higher and effective pathogen inhibition against MTB strain. In our previous report, we have reported that nanoparticulate delivery of bioactive agents enhances the effectivity due to slow and sustained release (26).

Fig. 7 Ex-vivo hemolytic study of polymers (HPMA, PLGA), lecithin, pure RMP, HP-NPs and HPR-NPs.



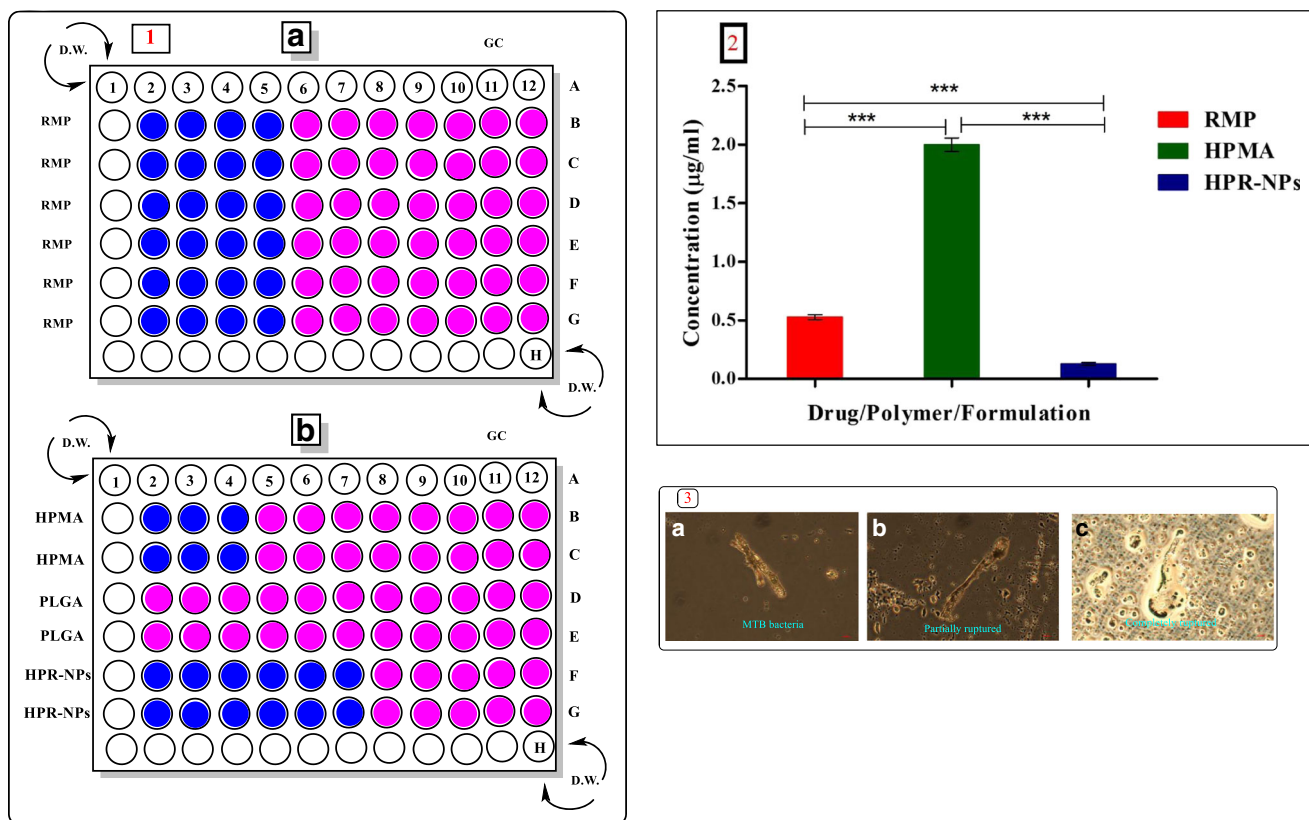


Fig. 8 (1) Pathogen inhibition studies for determination of MIC value of drugs and formulations by MABA (Microplate-Based Alamar Blue Assay) [A] effect of pure RMP on sensitive stain and [B] Effect of HPMA co-polymer, PLGA and HPR-NPs. (Pink colour showed the growth of bacteria and blue colour showed no growth of bacteria). (2) Minimum inhibitory concentration of RMP (red), HPMA co-polymer (green), RMP loaded HPMA-PLGA NPs (blue) against a sensitive *M. tuberculosis*. Values represents mean \pm SD ($n = 3$) [RMP, HPMA, HPR-NPs]. (3) Microscopic images of *M. tuberculosis* at different concentration of formulation as well as pure drugs at 40X. [(a) Growth of *M. tuberculosis* without treatment (b) pure RMP treated (c) HPR-NPs].

CONCLUSIONS

This study reports a novel approach for delivering anti-TB drug RMP by HP-NPs. The prepared HPR-NPs were not only able to solve the solubility issue of RMP but equally able to reduce the toxicity and to impart boosted cytotoxicity against drug sensitive MTB strain. The drug loading as well as entrapment efficiency were high enough that the robust method can be transformed into pilot batches in future. Interestingly, apart from increasing 65 fold the aqueous solubility; initial limited biocompatibility studies the nanoparticles were safe enough to be delivered in biological milieu in future studies. *In-vitro* MABA study revealed four fold higher anti-TB activity against MTB strain, which was an effective outcome of our study. Hence, it can be proved that co-polymeric NPs drug delivery can be an effective strategy to deliver hydrophobic anti-TB drug RMP. Additionally, use of HPMA as an established polymer for controlled release, also showed the potential for anti-TB drug delivery. This is one of few studies in which, the delivery of anti-TB drug has been attempted using HPMA copolymer. Conclusively, we may say that

nano-constructed PNP may improve the delivery of the anti-TB agent RMP.

ACKNOWLEDGMENTS AND DISCLOSURES

The authors acknowledge the financial support from the Rajasthan Department of Science and Technology, Jaipur India and Department of Science and Technology, New Delhi, India through DST Start up Research Grant (Young Scientists) to Dr. Umesh Gupta. Authors would also like to acknowledge Indian Council of Medical Research (ICMR) for providing facilities at JALMA, Agra, India. The authors declare no competing financial interest.

Publisher's Note Springer Nature remains neutral with regard to jurisdictional claims in published maps and institutional affiliations.

REFERENCES

1. World Health Organization Treatment of tuberculosis: guidelines for national programmes Geneva: WHO Global Tuberculosis Report 2017.

2. Sosnik A, Carcaboso R, Glisoni M, Chiappetta MD. New old challenges in tuberculosis: potentially effective nanotechnologies in drug delivery. *Adv Drug Deliv Rev.* 2010;62:547–59.
3. World Health Organization Communicable Diseases Cluster: Fixed-dose combination tablets for the treatment of tuberculosis 1999.
4. Mitchison DA. Role of individual drug in chemotherapy of tuberculosis. *Int J Tuberc Lung Dis.* 2000;4:790–800.
5. Joshi JM. Tuberculosis chemotherapy in the 21 century: Back to the basics. *Lung India.* 2011;28:193–200.
6. Zhang Y, Yew WW. Mechanisms of drug resistance in *Mycobacterium tuberculosis*. *Int J Tuberc Lung Dis.* 2009;13:1320–30.
7. Ain QU, Sharma S, Khuller GK, Garg SK. Alginate-based oral drug delivery system for tuberculosis: pharmacokinetic and therapeutic effects. *J Antimicrob Chemother.* 2003;51:931–8.
8. Labana S, Pandey R, Sharma S, Khuller GK. Chemotherapeutic activity against murine tuberculosis of once weekly administered drugs (INH and RMP) encapsulated in liposomes. *Int J Antimicrob Agents.* 2002;20:301–4.
9. Emerich DF, Thanos CG. Targeted nanoparticle-based drug delivery and diagnosis. *J Drug Target.* 2007;15:163–83.
10. Desjardins M, Griffiths G. Phagocytosis: latex leads the way. *Curr Opin Cell Biol.* 2003;15:498–503.
11. Pandey R, Khuller GK. Nanotechnology based drug delivery system(s) for the management of tuberculosis. *Indian J Exp Biol.* 2006;44:357–66.
12. Pandey R, Khuller GK. Chemotherapeutic potential of alginate-chitosan microspheres as anti-tubercular drug carriers. *J Antimicrob Chemother.* 2004;53:635–40.
13. Danhier F, Ansorena E, Silva JM, Coco R, Breton AL, Preat V. PLGA-based nanoparticles: an overview of biomedical applications. *J Control Release.* 2012;161:505–22.
14. Kopecek J, Kopeckova P, Minko T, Lu Z. HPMA copolymer-anticancer drug conjugates: design activity and mechanism of action. *Eur J Pharm Biopharm.* 2000;50:61–81.
15. Duncan R. Designing polymer conjugates as lysosomotropic nanomedicines. *Biochem Soc Trans.* 2007;35:56–60.
16. Rihova B, Ulbrich K, Kopecek J, Mancal P. Immunogenicity of N-(2-hydroxypropyl)-methacrylamide copolymers-potential hapten or drug carriers. *Folia Microbiol.* 1983;28:217–27.
17. Ulbrich K, Subr V, Strohalm J, Plocova D, Jelinkova M, Rihova B. Polymeric drugs based on conjugates of synthetic and natural macromolecules synthesis and physico-chemical characterization. *J Control Release.* 2000;64:63–79.
18. Wang D, Kopeckova JP, Minko T, Nanayakkara V, Kopecek J. Synthesis of starlike N-(2-hydroxypropyl) methacrylamide copolymers: potential drug carriers. *Biomacromolecules.* 2000;1:313–9.
19. Dvorak M, Kopeckova P, Kopecek J. High-molecular weight HPMA copolymer-adriamycin conjugates. *J Control Release.* 1999;60:321–32.
20. Chytil P, Etrych T, Kriz J, Subr V, Ulbrich K. N-(2-Hydroxypropyl) methacrylamide-based polymer conjugates with pH-controlled activation of doxorubicin for cell-specific or passive tumour targeting synthesis by RAFT polymerisation and physico-chemical characterization. *Eur J Pharm Sci.* 2010;41:473–82.
21. Chan JM, Zhang L, Yuet KP, Liao G, Rhee JW, Langer R, *et al.* PLGA-*lecithin*-PEG core-shell nanoparticles for controlled drug delivery. *Biomaterials.* 2009;30:1627–34.
22. Tomcin S, Kelsch A, Staff RH, Landfester K, Zentel R, Mailander V. HPMA-based block copolymers promote differential drug delivery kinetics for hydrophobic and amphiphilic molecules. *Acta Biomater.* 2015;35:12–22.
23. Vandervoort J, Ludwig A. Preparation and evaluation of drug-loaded gelatin nanoparticles for topical ophthalmic use. *Eur J Pharm Biopharm.* 2004;57:251–26.
24. Song H, Geng H, Ruan J, Wang K, Bao CN, Wang J, *et al.* Development of Polysorbate 80/phospholipid mixed micellar formation for docetaxel and assessment of its in vivo distribution in animal models. *Nanoscale Res Lett.* 2011;6:354.
25. Singhai AK, Jain S, Jain NK. Evaluation of an aqueous injection of Ketoprofen. *Pharmaz.* 1997;52:149–51.
26. Franzblau SG, Witzig RS, Mdaughlin JC, Torres P, Madico G, Hernandez A, *et al.* Rapid low-technology MIC determination with clinical *Mycobacterium tuberculosis* isolates by using the microplate Alamar blue assay. *J Clin Microbiol.* 1998;362–6.
27. Kalluru R, Fenaroli F, Westmoreland D, Ulanova L, Maleki A, Roos N, Madsen P, Koster G, Egge-Jacobsen W, Wilson S, Roberg-Larsen H, Khuller GK, Singh A, Nystrom B and Griffiths G. Poly(lactide-co-glycolide)-rifampicin nanoparticles efficiently clear *Mycobacterium bovis* BCG infection in macrophages and remain membrane-bound in phago-lysosomes. *J Cell Sci.* 2013;126:3034–54.
28. Kopeckej J, Copolymers KPHPMA. Origins early developments present and future. *Adv Drug Deliv Rev.* 2010;62:122–49.
29. Khan I, Gothwal A, Sharma AK, Qayumb A, Singh SK, Gupta U. Biodegradable nano-architectural PEGylated approach for the improved stability and anticancer efficacy of bendamustine. *Int J Biol Macromol.* 2016;92:1242–51.
30. Pelizza G, Nebuloni M, Ferrari P, Gallo GG. Polymorphism of rifampicin II. *Farmacol.* 1977;32:471–81.
31. Jindal KC, Chaudhary RS, Singla AK, Gangwal SS, Khanna S. Dissolution test methods for rifampicin-isoniazid fixed dose formulations. *J. Pharm Biomed Anal.* 1995;57:420–2.
32. Woo J, Cheung W, Chan R, Chan HS, Cheng A, Chan K. In vitro binding characteristics of isoniazid, rifampicin and pyrazinamide to whole plasma, albumin and α -1-acid glycoprotein. *Clin Biochem.* 1996;29:175–7.
33. Bergogne-Berezin E. Clinical role of protein binding of quinolones. *Clin Pharmacokinet.* 2002;41:741–50.
34. Wise R. Protein binding of beta-lactams: the effects on activity and pharmacology particularly tissue penetration II studies in man. *J Antimicrob Chemother.* 1983;12:105–18.
35. Costa P and Lobo JMS. Modeling and comparison of dissolution profiles. *Eur J Pharm Sci* 2001;13:123–33.
36. Nan A, Nanayakkara NP, Walker LA, Yardley V, Croft SL, Ghandehari H. N-(2-hydroxypropyl)methacrylamide (HPMA) copolymers for targeted delivery of 8-aminoquinoline antileishmanial drugs. *J Control Release.* 2001;77:233–43.